PHYSICAL REVIEW A

GENERAL PHYSICS

THIRD SERIES, VOL. 5, NO. 3 MARCH 1972

Atomic Vacancy Distributions Produced by Inner-Shell Ionization*

P. Venugopala Rao,† Mau Hsiung Chen, and Bernd Crasemann

Department of Physics, University of Oregon, Eugene, Oregon 97403

(Received 3 September 1971)

Average L- and M-shell–vacancy distributions produced in the deexcitation of atoms that have been singly ionized in the K shell or one of the L subshells are derived from a comprehensive set of available experimental and theoretical data on radiative- and Auger-transition rates. The data are supplemented by new calculations in j-j coupling from nonrelativistic screened hydrogenic wave functions of the following radiationless transition rates: K-LL, K-LM, and K-LN for selected elements with $20 \leq Z \leq 81$, and L_i-MM, L_i-MX, and L_i-XY for $26 \leq Z \leq 93$. Experimental and theoretical data on Auger- and radiative-transition probabilities are critically compared. Auger-electron intensity ratios and $K\alpha_2/K\alpha_1$ and $K\beta/K\alpha$ x-ray intensity ratios from a best fit to experimental data are tabulated for even atomic numbers from 20 to 94. The probability, per initial K vacancy, of vacancy production in each L_i subshell is derived from experimental data and tabulated for $20 \leq Z \leq 94$; components due to Auger and x-ray transitions are listed separately. These probabilities agree well with purely theoretical vacancy distributions also derived here. The probability of M-shell–vacancy production in the decay of K and L_i vacancies is derived from theory and tabulated for selected atoms with $16 \leq Z \leq 93$.

I. INTRODUCTION

When an atom has been ionized in an inner shell, it is deexcited through radiative or Auger transitions; owing to the latter, a multiplication of vacancies takes place. The average characteristics of such vacancy cascades are important for the experimental determination of fluorescence yields in cases where individual x-ray lines cannot be resolved with coincidence spectrometers. Knowledge of average vacancy distributions is also important for the study of such processes as nuclear electron capture, the internal conversion of γ rays, the photoelectric effect, and generally, whenever primary vacancies produced in outer shells must be distinguished from multiple ionization due to the decay of an inner vacancy. In the present paper, we draw upon existing data from Auger-electron spectroscopy and x-ray intensity measurements, supplemented by theoretical radiative- and radiationless-transition probabilities, to derive average L- and M-shell–vacancy distributions following K ionization, and M-vacancy distributions following ionization of any one of the L subshells.

II. BASIC RELATIONSHIPS

Following Listengarten,[1] Wapstra *et al.*,[2] and Fink *et al.*,[3] we denote by n_{KL_i} the average number of primary L_i-subshell vacancies produced in the decay of one K vacancy through radiative transitions and through Auger transitions of the types K-L_iL_j and K-L_iX. Excluded from this definition are additional L vacancies produced through Coster-Kronig transitions of the type L_i-L_jX, hence the word "primary" in the preceding sentence.

The quantities n_{KL_i} are related as follows to the pertinent radiative K-shell partial widths $\Gamma_R(KL_i)$, radiationless partial widths $\Gamma_A(KL_iL_j)$ and $\Gamma_A(KL_iX)$, and the total K-level width $\Gamma(K)$:

$$n_{KL_1}=\frac{\Gamma_R(KL_1)}{\Gamma(K)}+\frac{2\Gamma_A(KL_1L_1)+\Gamma_A(KL_1L_2)+\Gamma_A(KL_1L_3)+\Gamma_A(KL_1X)}{\Gamma(K)}=n_{KL_1}(R)+n_{KL_1}(A)\,, \tag{1}$$

$$n_{KL_2}=\frac{\Gamma_R(KL_2)}{\Gamma(K)}+\frac{2\Gamma_A(KL_2L_2)+\Gamma_A(KL_1L_2)+\Gamma_A(KL_2L_3)+\Gamma_A(KL_2X)}{\Gamma(K)}=n_{KL_2}(R)+n_{KL_2}(A)\,, \tag{2}$$

$$n_{KL_3}=\frac{\Gamma_R(KL_3)}{\Gamma(K)}+\frac{2\Gamma_A(KL_3L_3)+\Gamma_A(KL_1L_3)+\Gamma_A(KL_2L_3)+\Gamma_A(KL_3X)}{\Gamma(K)}=n_{KL_3}(R)+n_{KL_3}(A)\ . \tag{3}$$

Here, X symbolizes $M, N, O, \ldots$; $n_{KL_i}(R)$ stands for the contribution to n_{KL_i} due to radiative transitions; and $n_{KL_i}(A)$ denotes the contribution from Auger transitions. The average vacancy numbers n_{KL_i} can therefore be derived from theoretical partial widths. Pertinent radiative widths have recently been calculated by Scofield[4]; Auger widths for the transitions with which we are concerned here have been calculated by Kostroun, Chen, and Crasemann[5–7] and by McGuire.[8–10]

We define n_{KM} as the average total number of primary M-shell vacancies produced when a K vacancy decays through a radiative K-M transition or through an Auger transition of the type K-LM, K-MM, or K-MX. Specifically excluded from n_{KM} are M vacancies produced in two-step processes in which the decay of a K vacancy first leads to production of an L vacancy which then decays producing one or more M vacancies. In terms of partial widths, the average number of primary M_i-subshell vacancies produced per K-vacancy decay is

$$n_{KM_i}=\frac{\Gamma_R(KM_i)+2\Gamma_A(KM_iM_i)+\Gamma_A(KLM_i)+\Gamma_A(KM_iX)}{\Gamma(K)}\ , \tag{4}$$

where X stands for M_j $(j\neq i)$, N, O, $\ldots$.

The average number of M_i-subshell vacancies produced in the decay of an L_j vacancy is the sum of the number $n_{L_jM_i}(R)$ of vacancies produced through L_j-M_i radiative transitions, the number $n_{L_jM_i}(A)$ of vacancies produced through L_j-M_iM and L_j-M_iX Auger transitions, and the number $n_{L_jM_i}(CK)$ of vacancies due to Coster-Kronig transitions of the type L_j-LM_i. These three terms are given by the following equations:

$$n_{L_jM_i}(R)=\Gamma_R(L_jM_i)/\Gamma(L_j)\ , \tag{5}$$

$$n_{L_jM_i}(A)=\frac{2\Gamma_A(L_jM_iM_i)+\Gamma_A(L_jM_iX)}{\Gamma(L_j)}\ ,\quad X=M_j\ (j\neq i),\ N,\ O, \tag{6}$$

$$n_{L_jM_i}(CK)=\Gamma_A(L_jL_kM_i)/\Gamma(L_j)\ ,\quad k>j\ . \tag{7}$$

The L_j-L_kM_i Coster-Kronig transitions $(j=1,\ 2)$ occur only in regions of the periodic table where the binding-energy difference between the L_k subshell (in the presence of an M_i vacancy) and the L_j subshell exceeds the M_i binding energy.

The average number of M vacancies produced in the decay of an L_j-subshell vacancy is

$$n_{L_jM}=\sum_i n_{L_jM_i}\ . \tag{8}$$

It should be noted that we have excluded M_i vacancies due to the decay of L_k vacancies produced by transitions of the type L_j-L_kM_i; in this respect, our definition differs from the approach of McGuire.[9]

In some practical situations, the quantity of interest is the *total* average number of M_i-subshell vacancies that arise when a K vacancy decays. This number includes primary vacancies as well as vacancies produced through cascade (two- and three-step) processes; we denote it by $\bar{n}_{KM_i}$. Similarly, we define $\bar{n}_{L_jM_i}$ as the total average number of M_i vacancies produced in the decay of an L_j vacancy, including vacancies that arise from the decay of the second L vacancy due to L_j-L_kX Coster-Kronig transitions. The quantities $\bar{n}$ are easily calculated

TABLE I. Theoretical K-LL Auger-transition probabilities in j-j coupling (in multiples of 10^{-3} a.u.).[a]

Z	Element	K-L_1L_1	K-L_1L_2	K-L_1L_3	K-L_2L_2	K-L_2L_3	K-L_3L_3	Total
20	Ca	2.881	2.434	4.860	0.171	4.469	2.572	17.387
30	Zn	2.694	2.654	5.291	0.261	6.578	3.794	21.272
35	Br	2.667	2.683	5.344	0.281	7.143	4.120	22.238
40	Zr	2.637	2.689	5.349	0.310	7.630	4.396	23.011
47	Ag	2.601	2.698	5.354	0.333	8.127	4.669	23.782
49	In	2.592	2.701	5.356	0.339	8.250	4.735	23.976
50	Sn	2.588	2.702	5.355	0.341	8.305	4.764	24.055
52	Te	2.581	2.701	5.350	0.346	8.406	4.817	24.201
55	Cs	2.571	2.702	5.344	0.354	8.550	4.892	24.413
60	Nd	2.550	2.701	5.332	0.363	8.750	4.986	24.682
70	Yb	2.511	2.688	5.279	0.377	8.994	5.079	24.928
71	Lu	2.507	2.687	5.273	0.378	9.010	5.082	24.937
75	Re	2.493	2.683	5.251	0.382	9.061	5.088	24.958
78	Pt	2.482	2.677	5.230	0.384	9.081	5.080	24.934
80	Hg	2.476	2.673	5.215	0.385	9.088	5.070	24.907
81	Tl	2.473	2.672	5.208	0.386	9.088	5.064	24.891

[a] 1 a.u. $=4.134\times10^{16}\ \mathrm{sec}^{-1}=27.212\ \mathrm{eV}/\hbar$.

TABLE II. Theoretical *K-LM* Auger-transition probabilities in *j-j* coupling (in multiples of 10^{-3} a.u.).

Z	Element	K-L_1M_1	K-L_1M_2	K-L_1M_3	K-L_1M_4	K-L_1M_5	K-L_2M_1	K-L_2M_2	K-L_2M_3	K-L_2M_4	K-L_2M_5	K-L_3M_1	K-L_3M_2	K-L_3M_3	K-L_3M_4	K-L_3M_5	Total
20	Ca	1.374	0.199	0.397			0.732	0.026	0.362			1.462	0.361	0.413			5.326
30	Zn	1.363	0.273	0.547	0.002	0.003	0.840	0.053	0.680	0.002	0.008	1.674	0.678	0.783	0.010	0.011	6.927
35	Br	1.373	0.326	0.652	0.009	0.013	0.832	0.071	0.867	0.009	0.031	1.655	0.863	1.002	0.039	0.040	7.782
40	Zr	1.372	0.376	0.752	0.016	0.024	0.814	0.087	1.048	0.016	0.060	1.617	1.041	1.213	0.074	0.076	8.586
47	Ag	1.361	0.430	0.859	0.026	0.039	0.788	0.106	1.246	0.027	0.102	1.561	1.235	1.442	0.125	0.128	9.475
49	In	1.357	0.442	0.883	0.029	0.043	0.781	0.111	1.294	0.031	0.114	1.548	1.282	1.497	0.140	0.143	9.695
50	Sn	1.356	0.448	0.894	0.030	0.045	0.778	0.113	1.317	0.032	0.119	1.541	1.304	1.523	0.147	0.150	9.797
52	Te	1.352	0.459	0.916	0.033	0.049	0.772	0.117	1.360	0.035	0.130	1.527	1.346	1.572	1.160	0.163	9.991
55	Cs	1.346	0.474	0.946	0.036	0.054	0.762	0.123	1.421	0.039	0.146	1.506	1.403	1.640	0.178	0.181	10.255
60	Nd	1.334	0.495	0.987	0.042	0.062	0.748	0.131	1.507	0.045	0.171	1.475	1.485	1.735	0.208	0.211	10.636
70	Yb	1.309	0.522	1.040	0.050	0.075	0.722	0.143	1.627	0.055	0.212	1.417	1.594	1.860	0.256	0.257	11.139
71	Lu	1.306	0.524	1.044	0.050	0.076	0.720	0.144	1.637	0.056	0.215	1.412	1.602	1.869	0.259	0.260	11.170
75	Re	1.296	0.531	1.058	0.053	0.079	0.712	0.148	1.669	0.058	0.228	1.392	1.629	1.899	0.272	0.272	11.292
78	Pt	1.288	0.536	1.066	0.054	0.081	0.705	0.150	1.689	0.060	0.235	1.376	1.644	1.915	0.280	0.270	11.358
80	Hb	1.283	0.538	1.071	0.055	0.083	0.701	0.151	1.700	0.061	0.240	1.366	1.652	1.923	0.285	0.283	11.392
81	Tl	1.281	0.540	1.073	0.056	0.083	0.699	0.151	1.705	0.061	0.242	1.361	1.655	1.927	0.287	0.285	11.406

TABLE III. Theoretical *K-LN* Auger-transition probabilities in *j-j* coupling (in multiples of 10^{-3} a.u.)

Z	Element	K-L_1N_1	K-L_1N_2	K-L_1N_3	K-L_1N_4	K-L_1N_5	K-L_2N_1	K-L_2N_2	K-L_2N_3	K-L_2N_4	K-L_2N_5	K-L_3N_1	K-L_3N_2	K-L_3N_3	K-L_3N_4	K-L_3N_5	Total
20	Ca	0.232					0.138					0.276					0.646
30	Zn	0.190					0.144					0.287					0.621
35	Br	0.334	0.010	0.019			0.249	0.002	0.031			0.495	0.031	0.035			1.206
40	Zr	0.421	0.033	0.066	0.000	0.000	0.305	0.008	0.105	0.000	0.000	0.605	0.104	0.121	0.000	0.000	1.768
47	Ag	0.462	0.053	0.105	0.000	0.000	0.326	0.014	0.172	0.001	0.002	0.644	0.170	0.197	0.002	0.002	2.150
49	In	0.470	0.059	0.117	0.001	0.001	0.329	0.016	0.192	0.001	0.003	0.650	0.189	0.220	0.004	0.004	2.256
50	Sn	0.475	0.062	0.124	0.001	0.001	0.331	0.017	0.204	0.001	0.004	0.653	0.201	0.234	0.005	0.005	2.318
52	Te	0.483	0.070	0.239	0.001	0.002	0.333	0.019	0.229	0.002	0.006	0.657	0.225	0.262	0.008	0.008	2.444
55	Cs	0.488	0.081	0.162	0.002	0.003	0.336	0.023	0.271	0.003	0.010	0.660	0.266	0.310	0.012	0.013	2.640
60	Nd	0.498	0.091	0.183	0.003	0.004	0.335	0.026	0.303	0.004	0.014	0.657	0.297	0.347	0.018	0.019	2.799
70	Yb	0.497	0.102	0.203	0.004	0.006	0.329	0.029	0.343	0.006	0.021	0.641	0.333	0.390	0.025	0.027	2.956
71	Lu	0.497	0.103	0.206	0.004	0.006	0.329	0.030	0.348	0.006	0.022	0.639	0.338	0.395	0.026	0.028	2.977
75	Re	0.496	0.109	0.218	0.005	0.007	0.326	0.032	0.369	0.008	0.026	0.632	0.357	0.418	0.031	0.033	3.067
78	Pt	0.495	0.114	0.227	0.006	0.008	0.323	0.033	0.385	0.008	0.030	0.625	0.371	0.434	0.035	0.037	3.131
80	Hg	0.495	0.117	0.233	0.006	0.009	0.321	0.034	0.394	0.009	0.032	0.620	0.379	0.444	0.038	0.039	3.170
81	Tl	0.495	0.118	0.236	0.006	0.009	0.320	0.035	0.399	0.009	0.033	0.617	0.383	0.449	0.039	0.041	3.189

TABLE IV. Theoretical Auger-transition probabilities to the three L subshells, computed in j-j coupling (in multiples of 10^{-3} a.u.).

Z	Element	L_1-MM	L_1-MX	L_1-XY	L_2-MM	L_2-MX	L_2-XY	L_3-MM	L_3-MX	L_3-XY
26	Fe				44.618	2.863	0.0	45.627	2.920	0.0
28	Ni				45.343	3.314	0.0			
29	Cu				46.563	3.638	0.0	47.805	3.682	0.0
32	Ge				47.421	5.005	0.089			
33	As	36.609	6.484	0.260	47.815	7.561	0.263	49.481	7.752	0.280
34	Se				48.560	10.069	0.538			
35	Br				49.746	12.994	0.947			
36	Kr	37.732	14.138	1.197	50.927	16.162	1.486	52.781	16.960	1.590
37	Rb				51.362	18.561	1.923			
40	Zr	38.499	18.818	2.048	53.694	22.227	2.650	56.196	23.348	2.702
42	Mo	39.053	19.336	2.212	55.283	23.140	2.794	57.577	24.532	2.857
47	Ag	40.737	20.823	2.642	59.244	25.833	3.343	62.736	27.713	3.337
50	Sn	42.655	22.849	2.932	61.309	28.576	3.680			
51	Sb	41.726	23.924	3.182				65.985	32.422	4.419
56	Ba	40.972	28.492	4.624	63.528	33.576	5.465	68.269	40.670	6.513
60	Nd	43.428	28.840	4.502	65.751	37.481	5.658	72.007	41.778	6.490
65	Tb				66.185	39.623	6.977	74.864	45.094	7.601
67	Ho	44.063	30.352	4.928						
70	Yb	42.937	30.419	4.921						
74	W	44.334	31.413	4.956	68.030	41.289	6.517	78.561	48.672	8.007
80	Hg	44.251	31.688	5.499	67.961	43.059	6.910	80.784	52.181	8.779
85	At	43.932	32.191	5.609	67.571	44.223	7.349	82.496	55.178	9.620
93	Np				66.164	45.728	7.619	85.021	59.837	10.116

from the vacancy distributions n_{KL_i} and n_{LM} defined above and from the pertinent L-shell Coster-Kronig transition probabilities.[6,7,9] It should be noted, however, that the Coster-Kronig transition probabilities may in some cases be drastically different for an ion with a doubly ionized L shell, compared with the transition probability for an atom with a single L-shell vacancy. This is due to the fact that strong radiationless transitions that can occur in singly ionized atoms may be energetically forbidden in doubly ionized atoms.

III. THEORETICAL K AND L AUGER RATES

We compute Auger-transition rates to an initial K-shell vacancy as done by Kostroun *et al.*,[5] but in j-j coupling. Specially screened nonrelativistic hydrogenic wave functions are used to describe the initial- and final-state vacancies. Details of the calculation and an analytic expression for the radial matrix element are contained in Ref. 5. The angular factors in j-j coupling, for final vacancy configurations through $f_{7/2}f_{7/2}$, have been reported elsewhere.[11] Results are listed in Tables I–III.

Auger-transition rates to the three L subshells are listed in Table IV. These were computed in the course of fluorescence-yield calculations,[6,7] but had not been published. In Fig. 1, $(L_iMX)/(L_i\text{-}MM)$ and $(L_i\text{-}XY)/(L_i\text{-}MM)$ ratios are plotted as functions of atomic number.

In Sec. IV, we compare suitable ratios of Auger-transition probabilities from the present work and from the calculations of Asaad,[12,13] Mehlhorn and Asaad,[14] Ramsdale,[15] and McGuire[8] with experimental data.

IV. COMPARISON WITH EXPERIMENT

Experimental information on Auger-transition rates is available in the form of intensity ratios. In particular, relative intensities have been measured for (a) major K-Auger-electron groups, such as K-LL, K-LX, and K-XY; (b) K-L_iL_j Auger lines; and (c) K-L_iX lines. A thorough search of the literature reveals that suitable experimental information is contained in Refs. 16–96.

A. Comparison of K-LL Auger-Electron Intensity Ratios b_i

We define b_i as the probability of producing an L_i vacancy per K-LL Auger transition. For example, for the L_1 subshell we have, in terms of intensities I or widths Γ,

$$b_1 = \frac{2I(KL_1L_1) + I(KL_1L_2) + I(KL_1L_3)}{I(KLL)} = \frac{2\Gamma(KL_1L_1) + \Gamma(KL_1L_2) + \Gamma(KL_1L_3)}{\Gamma(KLL)} . \qquad (9)$$

In Figs. 2–4 we compare the measured ratios b_i derived from information contained in Refs. 16–96 with theoretical ratios calculated from nonrelativistic wave functions in j-j coupling in the present work, by Asaad,[12] and by McGuire[8]; in intermedi-

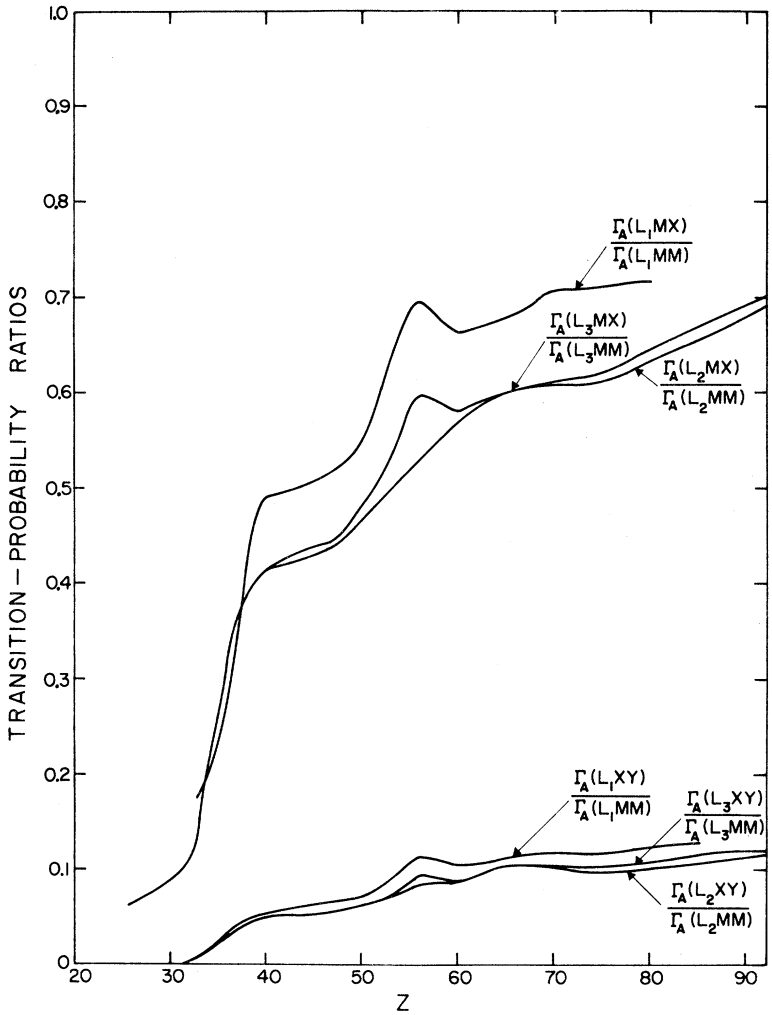

FIG. 1. Ratios of theoretical Auger-transition probabilities to the three L subshells, as functions of atomic number.

ate coupling by Asaad[12]; in intermediate coupling with configuration mixing by Asaad[13] and by Mehlhorn and Asaad[14]; and from relativistic wave functions in j-j coupling by Ramsdale. Clearly, none of the theoretical estimates of the ratios b_i agree well with experiment over the entire range of atomic numbers. Only the relativistic calculations of Ramsdale[15] agree fairly well with measurements at high atomic numbers ($Z > 55$). However, at lower Z where the Auger effect plays a dominant role in creating L vacancies, the relativistic calculations are far off. McGuire's b_1 agrees reasonably well in magnitude for $20 < Z < 40$, and some of the nonrelativistic results for b_2 and b_3 follow the trend of measured ratios, but they obviously are not sufficiently accurate for the purpose of calculating vacancy distributions.[97] A best fit to the experimental data, indicated by the broken curves in Figs. 2–4, is therefore used below in the calculation of n_{KL_i}.

B. Comparison of *K-LL*, *K-LX*, and *K-XY* Auger-Transition Probabilities

All available experimental data[16–96] on the Auger-electron intensity ratios $I(KXY)/I(KLL)$ and $I(KLX)/I(KLL)$ are plotted in Fig. 5. Earlier summaries of these ratios have been prepared by Listengarten,[1] Wapstra *et al.*,[2] Hörnfeldt,[98] Gray,[54] and Erman *et al.*[41] There is considerable scatter in the experimental points, overshadowing the errors in individual results; error flags have therefore been omitted from Fig. 5. Theoretical ratios based on the present work and on the calculations of McGuire[8,99] are indicated; these predict a plateau in the region $18 \leq Z \leq 28$ because $3d$ electrons contribute relatively little to the K Auger-transition rates. Unfortunately, experimental information is lacking in this region. Thus, in fitting a smooth curve to the data, this aspect has been ignored. Values read from the fitted curve (broken line in Fig. 5) in this region should therefore be used with

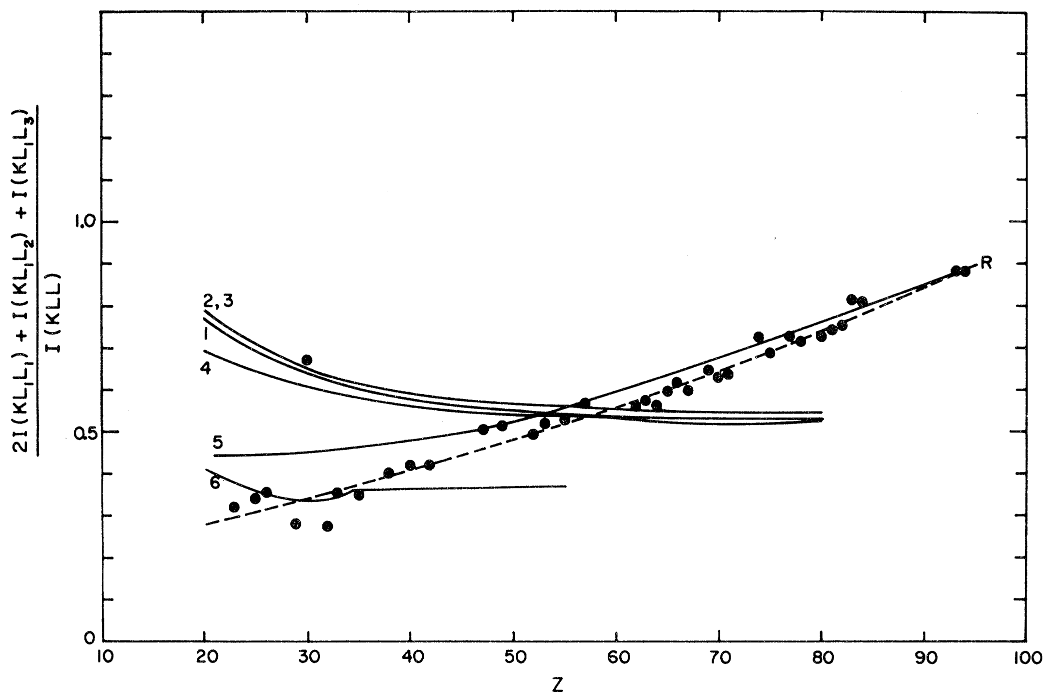

FIG. 2. Probability b_1 of L_1-vacancy production per *K-LL* Auger transition, as a function of atomic number. The points are experimental ratios from Refs. 16–95; probable errors range from 10 to 15%. Solid curves indicate theoretical ratios: 1, present work; 2, nonrelativistic calculations in *j-j* coupling by Asaad (Ref. 12); 3, nonrelativistic calculation in intermediate coupling by Asaad (Ref. 12); 4, nonrelativistic calculations in intermediate coupling with configuration mixing by Asaad (Ref. 13) and by Mehlhorn and Asaad (Ref. 14); 5, relativistic calculation in *j-j* coupling by Ramsdale (Ref. 15); and 6, nonrelativistic calculations by McGuire in *LS* coupling (Ref. 8). The broken curve is a least-squares fit to the experimental points.

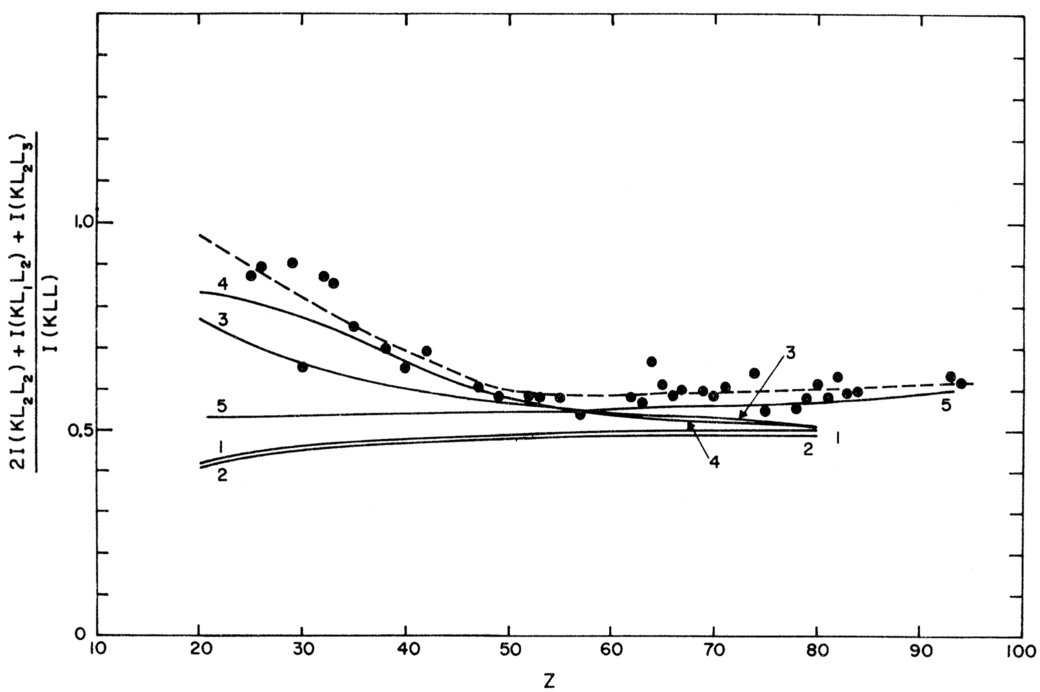

FIG. 3. Probability b_2 of L_2-vacancy production per *K-LL* Auger transition, as a function of atomic number. The points are experimental ratios from Refs. 16–96; probable errors are 10–15%. Solid curves indicate theoretical ratios, keyed as in Fig. 1. The broken curve is a least-squares fit to the measured points.

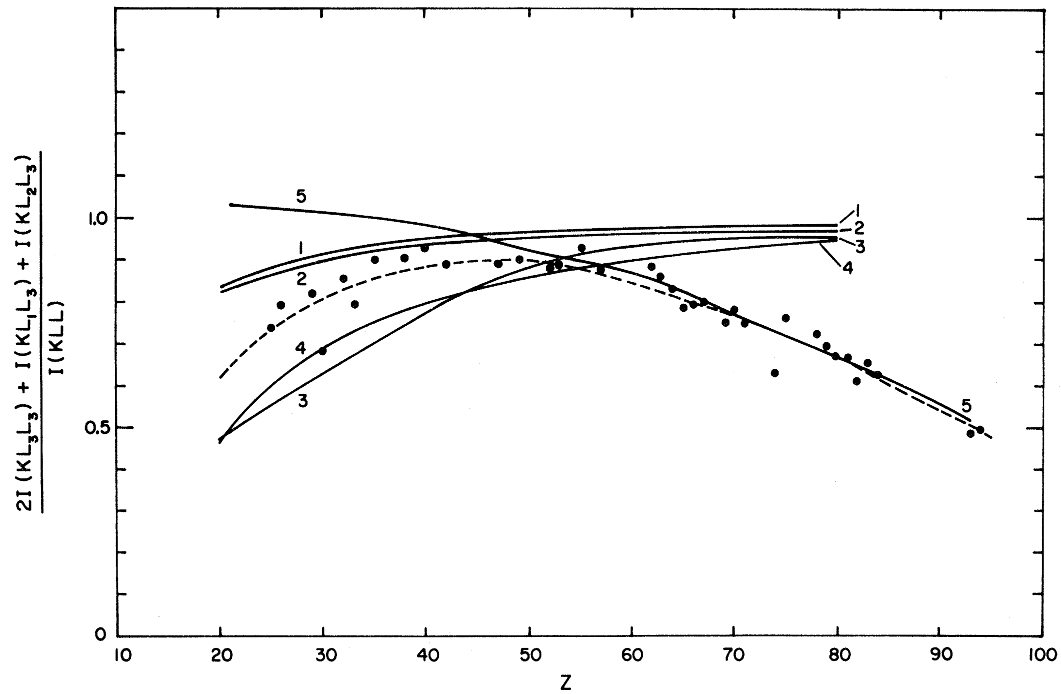

FIG. 4. Probability b_3 of L_3-vacancy production per K-LL Auger transition, as a function of atomic number. The points represent measured ratios from Refs. 16–96 with probable errors of 10–15%. Theoretical ratios are indicated by solid curves, keyed as in Fig. 1. The broken curve is a least-squares fit to the experimental points.

caution. The K-XY transition rates are approximately ten times smaller than the K-LX rates, hence the large uncertainties in K-XY rates do not significantly impair the calculation of vacancy distributions n_{KL}.

C. Comparison of K-L_1X, K-L_2X, and K-L_3X Auger-Transition Probabilities

Experimental data on Auger transitions to individual L subshells are limited in number and also in reliability, owing to difficulty in resolving electron lines. Only for $Z=35$, 47, 49, 52, 55, 71, 75, 78, 80, and 81 could relative K-L_iX intensities be deduced from data in Refs. 16–96. In some cases, measured intensities had to be allotted among several unresolved lines. Experimental ratios are plotted in Fig. 6; a best fit to the data and theoretical predictions based on the present work are also indicated. The best fit to the experimental data is used below for the calculation of L-vacancy distributions. It should be noted that earlier estimates by Listengarten,[1] based on fewer experimental data, do not agree well with the present fit.

D. Comparison of K-LM and K-LN Auger-Transition Probabilities

The remarks in Sec. IV C concerning experimental data apply here as well. In Fig. 7, the few available measured ratios[16–96] are shown and compared with predictions from the present work and from that of Bhalla *et al.*,[15,100] and of Asaad and Burhop.[101] For comparison, Listengarten's estimates of average values[1] are also included.

In summary, a review of the data on Auger intensities indicates that further theoretical work is very much needed, especially for atomic numbers below $Z=55$ where radiationless transitions dominate in the deexcitation of K-shell vacancies. Consequently, we have used best fits to experimental data for the calculation of L-vacancy production following K Auger transitions, i.e., of $n_{KL_i}(A)$. However, experimental information on M-vacancy production is so scarce that we have had to rely on theoretical estimates alone. Most M vacancies are produced in Auger transitions to the L subshells. Experimental data are available for only nine elements[28,68,76,91,94,102–110] ($Z=49$, 52, 71, 78, 80, 81, 83, and 92). Published data on 8 other elements provide only qualitative information on Auger-electron intensities.[16,32,33,40,67,91,111–113] The spectra are complicated even at the highest atomic numbers; only major L_3-MM groups of relatively low energy are resolved. The high-energy end of the spectrum contains composite peaks that include contributions from transitions to the L_1 and L_2 subshells as well as from L_3-MN and L_3-NN transitions.

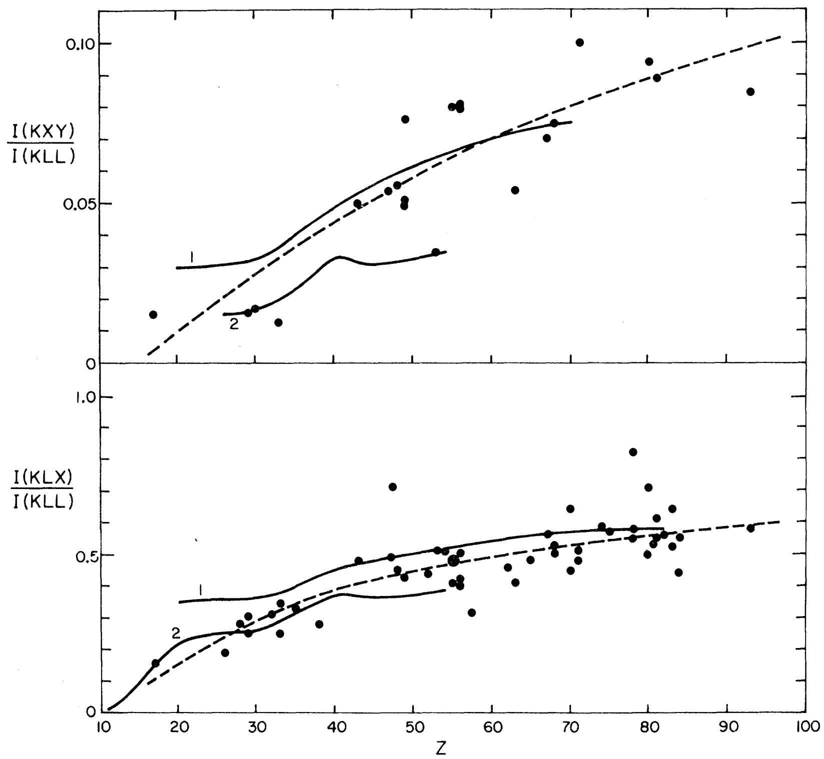

FIG. 5. Auger-electron intensity ratios $I(KXY)/I(KLL)$ and $I(KLX)/I(KLL)$, as functions of atomic number. The data points are from Refs. 16–96. Probable errors in the experimental KXY/KLL ratios range from 10% at high Z to 25% at low Z. Solid curves indicate theoretical predictions (curve 1) from the present work and (curve 2) from the calculations of McGuire (Refs. 8 and 99). The broken curves are best fits to the measured ratios.

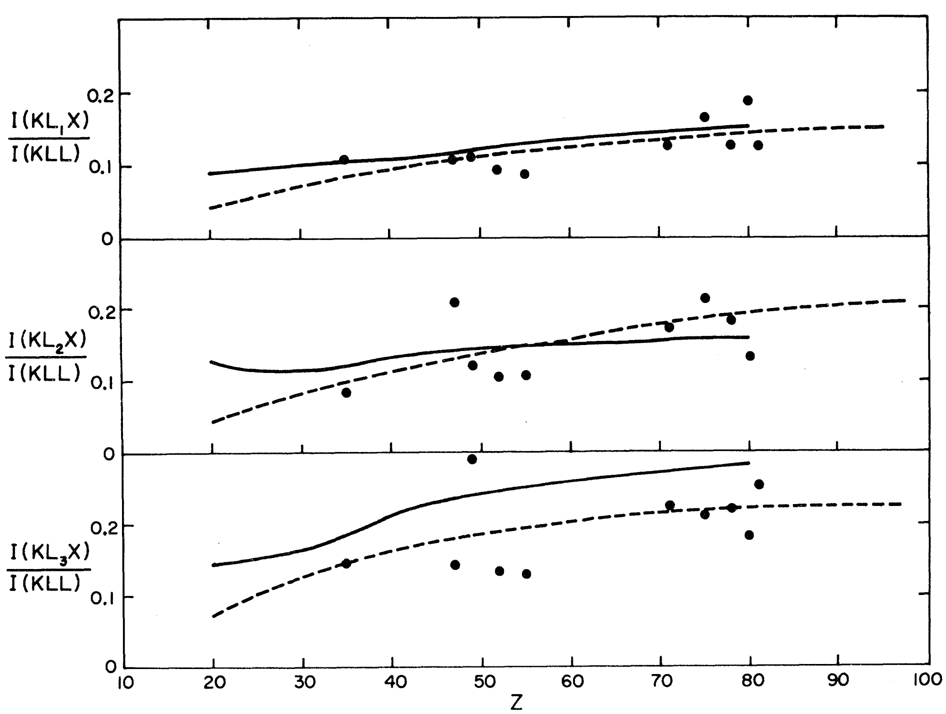

FIG. 6. Auger-elec'ron intensity ratios $I(KL_iX)/I(KLL)$. Experimental data points are from Refs. 16–96; probable errors are 5–10%. The solid curves represent theoretical predictions from the present work. The broken curves are best fits to the data.

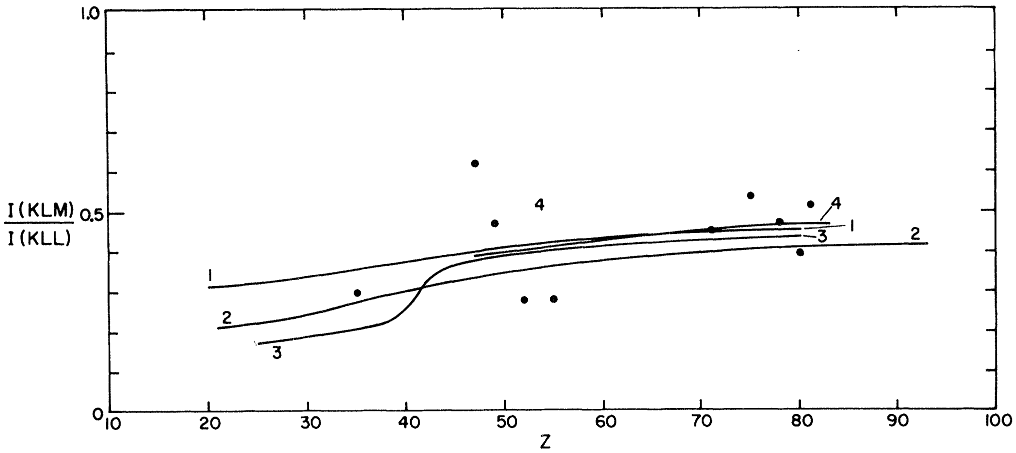

FIG. 7. Auger-electron intensity ratio $I(KLM)/I(KLL)$ as a function of atomic number. Experimental data (Refs. 16–96) are compared with predictions from the present calculations (curve 1), from the relativistic calculations of Bhalla, Rosner, and Ramsdale (Refs. 15 and 100; curve 2), and from the work of Asaad and Burhop (Ref. 101; curve 3). Curve 4 is the estimate of Listengarten (Ref. 1). Probable errors in the experimental ratios are ~20%.

V. RADIATIVE TRANSITION PROBABILITIES

Relative x-ray emission rates are required, in addition to Auger rates, to compute vacancy distributions. Theoretical radiative transition rates have recently been calculated by Scofield[4] and by Rosner and Bhalla,[114] with virtually identical results. A number of measurements of relative x-ray intensities have recently been performed with the aid of solid-state detectors.[115–127] In Fig. 8, we compare measured $K\alpha_2/K\alpha_1$ x-ray intensity ratios with the theoretical results of Scofield.[4] Clearly, there is very good agreement between theory and experiment over the entire range of atomic numbers. On the other hand, measured $K\beta/K\alpha$ x-ray intensity ratios consistently exceed theoretical values (Fig. 9). This discrepancy has already been pointed out by Rao *et al.*[125] For the calculation of vacancy distributions, we use a best fit to measured x-ray intensity ratios, also indicated in

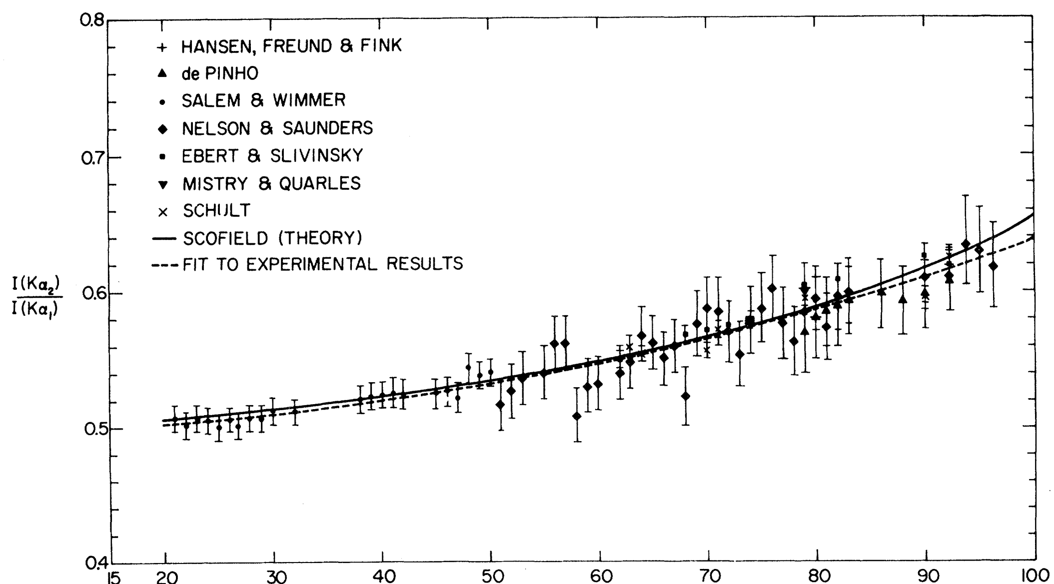

FIG. 8. $K\alpha_2/K\alpha_1$ x-ray intensity ratio as a function of atomic number. The measured points are from de Pinho (Ref. 120), Salem and Wimmer (Ref. 122), Nelson and Saunders (Ref. 115), Ebert and Slivinsky (Refs. 116 and 117), Mistry and Quarles (Refs. 123 and 124), and Schult (Ref. 121). The solid curve indicates the theoretical ratio computed by Scofield (Ref. 4); the broken curve is a least-squares fit to the experimental data.

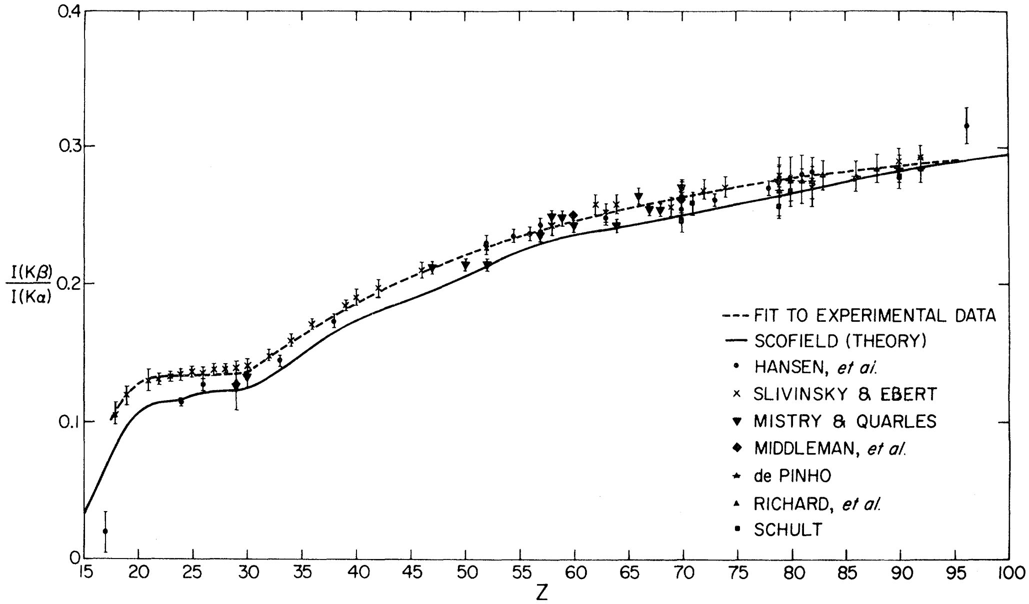

FIG. 9. $K\beta/K\alpha$ x-ray intensity ratio as a function of atomic number. Experimental data are from Hansen *et al.* (Refs. 118 and 119), Slivinsky and Ebert (Refs. 116 and 117), Mistry and Quarles (Refs. 123 and 124), Middleman *et al.* (Ref. 126), de Pinho (Ref. 120), Richard *et al.* (Ref. 127), and Schult (Ref. 121). The solid curve is the theoretical $K\beta/K\alpha$ ratio from the work of Scofield (Ref. 4), and the broken curve is a best fit to the experimental points.

Figs. 8 and 9.

VI. CALCULATION OF VACANCY DISTRIBUTIONS n_{KL_i}

For the purpose of computing average vacancy distributions n_{KL_i}, defined in Sec. II, we can express the Auger and radiative contributions $n_{KL_i}(A)$ and $n_{KL_i}(R)$ in terms of experimentally measured ratios. For example, the following relations hold for the L_2 subshell:

$$n_{KL_2}(R)=\omega_K\left(\frac{I(K\alpha_2)}{I(K\alpha_1)}\right)\left[\left(1+\frac{I(K\alpha_2)}{I(K\alpha_1)}\right)\left(1+\frac{I(K\beta)}{I(K\alpha)}\right)\right]^{-1}, \tag{10}$$

$$n_{KL_2}(A)=(1-\omega_K)\left(b_1+\frac{I(KL_2X)}{I(KLL)}\right)\left(1+\frac{I(KLX)}{I(KLL)}+\frac{I(KXY)}{I(KLL)}\right)^{-1}. \tag{11}$$

The pertinent Auger-electron intensity ratios, derived from the best fit to the experimental data,[16–96] are listed in Table V. The relevant x-ray intensity ratios from a best fit to measured quantities[115–127] are listed in Table VI. Fluorescence yields ω_K for the calculation of n_{KL_i} are taken from a best fit to selected "most reliable" experimental values.[128]

The average vacancy numbers n_{KL_i}, as defined in Sec. II, were calculated from the experimental Auger-electron and x-ray intensity ratios of Tables V and VI and are listed in Table VII for even atomic numbers $20 \leq Z \leq 94$. The quantities $n_{KL_1}(R)$ have been omitted; they are negligible throughout because the L_1-K electric dipole transition is forbidden.

Vacancy distributions $n_{KL}(A)$ and

$$n_{KL}(R)=n_{KL_2}(R)+n_{KL_3}(R)$$

computed from experimental data (Table VII) are compared in Fig. 10 with distributions derived purely from theory. The theoretical distributions were calculated from the Auger rates of the present work, the x-ray emission rates of Scofield,[4] and the K-shell fluorescence yields of Kostroun *et al.*[5] Agreement between theoretical and experimental $n_{KL}(R)$ is seen to be good; the slight discrepancy in $K\beta/K\alpha$ x-ray intensity ratios does not appear to contribute a significant error to $n_{KL}(R)$. The agreement between theory and experiment in the case of $n_{KL}(A)$ is remarkable, especially in view of the fact that relative Auger rates to the individual L subshells do not agree well (Sec. IV). The fact that theoretical total Auger rates are so close to measured rates is reassuring, since M-shell–vacancy distributions computed in Sec. VII must of necessity be based on theory alone, due to the dearth of experimental information (Sec. IV D).

VII. M-VACANCY PRODUCTION FOLLOWING DECAY OF K AND L VACANCIES

The probabilities $n_{KM}(A)$ and $n_{KM}(R)$ that a primary M-shell vacancy is produced in the radiationless or radiative decay of a K vacancy has been calculated from Scofield's x-ray emission rates[4]

TABLE V. Auger-electron intensity ratios derived from a least-squares fit to the experimental data of Refs. 16–96.

Z	b_1 [a]	b_2 [a]	b_3 [a]	$\frac{KL_1X}{KLL}$	$\frac{KL_2X}{KLL}$	$\frac{KL_3X}{KLL}$	$\frac{KLX}{KLL}$	$\frac{KXY}{KLL}$
20	0.281	0.972	0.614	0.046	0.042	0.074	0.161	0.0096
22	0.293	0.938	0.670	0.054	0.048	0.087	0.189	0.0135
24	0.305	0.906	0.716	0.062	0.054	0.098	0.215	0.0173
26	0.317	0.876	0.753	0.070	0.060	0.109	0.239	0.0210
28	0.329	0.846	0.783	0.078	0.065	0.119	0.262	0.0246
30	0.342	0.818	0.808	0.085	0.071	0.128	0.284	0.0280
32	0.355	0.791	0.828	0.081	0.075	0.138	0.304	0.0314
34	0.368	0.766	0.845	0.098	0.081	0.144	0.323	0.0347
36	0.382	0.741	0.858	0.105	0.085	0.152	0.342	0.0379
38	0.395	0.717	0.869	0.111	0.089	0.158	0.359	0.0410
40	0.409	0.695	0.878	0.116	0.094	0.165	0.375	0.0440
42	0.424	0.673	0.886	0.122	0.097	0.170	0.390	0.0470
44	0.438	0.652	0.892	0.127	0.101	0.176	0.404	0.0498
46	0.453	0.632	0.897	0.133	0.104	0.180	0.417	0.0526
48	0.468	0.613	0.901	0.138	0.107	0.185	0.430	0.0553
50	0.483	0.595	0.897	0.142	0.111	0.189	0.442	0.0579
52	0.499	0.580	0.888	0.146	0.114	0.193	0.453	0.0604
54	0.515	0.581	0.879	0.151	0.116	0.196	0.463	0.0629
56	0.531	0.583	0.869	0.154	0.119	0.200	0.473	0.0653
58	0.547	0.584	0.857	0.159	0.122	0.202	0.483	0.0677
60	0.564	0.586	0.845	0.163	0.124	0.206	0.492	0.0699
62	0.581	0.587	0.832	0.166	0.126	0.208	0.500	0.0721
64	0.598	0.589	0.817	0.170	0.128	0.211	0.508	0.0743
66	0.616	0.591	0.802	0.173	0.130	0.212	0.515	0.0764
68	0.633	0.592	0.786	0.176	0.132	0.214	0.522	0.0784
70	0.651	0.594	0.769	0.179	0.134	0.215	0.528	0.0804
72	0.670	0.596	0.751	0.182	0.135	0.218	0.535	0.0823
74	0.688	0.598	0.732	0.185	0.137	0.219	0.540	0.0841
76	0.707	0.599	0.712	0.187	0.138	0.220	0.546	0.0859
78	0.726	0.601	0.691	0.190	0.140	0.222	0.551	0.0877
80	0.746	0.603	0.669	0.192	0.142	0.223	0.556	0.0894
82	0.765	0.605	0.647	0.195	0.142	0.223	0.560	0.0911
84	0.785	0.607	0.623	0.197	0.143	0.225	0.565	0.0927
86	0.805	0.609	0.598	0.199	0.145	0.255	0.569	0.0942
88	0.826	0.611	0.572	0.201	0.145	0.226	0.572	0.0958
90	0.846	0.613	0.546	0.203	0.145	0.226	0.576	0.0972
92	0.867	0.615	0.518	0.205	0.147	0.227	0.579	0.0987
94	0.888	0.617	0.489	0.207	0.148	0.228	0.583	0.100

[a] As defined in Sec. IV A, b_i is the probability, per K-LL Auger transition, that an L_i vacancy is produced.

and the theoretical Auger-transition probabilities of the present work. The results are indicated in Table VIII, which also contains the theoretical probabilities $n_{L_iM}(A)+n_{L_iM}(CK)$ and $n_{L_iM}(R)$ for selected elements.

The predicted M-vacancy production due to radiative transitions can be compared with distributions calculated from measured fluorescence yields and x-ray intensity ratios. We have

$$n_{KM}(R)=\omega_K\frac{I(K\beta_1')}{I(K\alpha_1)}\left[\left(1+\frac{I(K\alpha_2)}{I(K\alpha_1)}\right)\left(1+\frac{I(K\beta)}{I(K\alpha)}\right)\right]^{-1} \qquad (12)$$

and

$$n_{L_iM}(R)=\omega_i/(1+s_i)\ , \qquad (13)$$

where s_i stands for x-ray branching ratios as defined by Venugopala Rao, Palms, and Wood[125]:

$$s_1=\frac{I(L_1\rightarrow N)+I(L_1\rightarrow 0)+\cdots}{I(L_1\rightarrow M)}=\frac{\text{Intensity of } L\gamma \text{ x rays originating from } L_1 \text{ vacancies}}{\text{Intensity of } L\beta \text{ x rays originating from } L_1 \text{ vacancies}}\ , \qquad (14)$$

$$s_2=\frac{I(L_2\rightarrow N)+I(L_2\rightarrow 0)+\cdots}{I(L_2\rightarrow M)}=\frac{\text{Intensity of } L\gamma \text{ x rays originating from } L_2 \text{ vacancies}}{\text{Intensity of } L\eta \text{ and } L\beta \text{ x rays originating from } L_2 \text{ vacancies}}\ , \qquad (15)$$

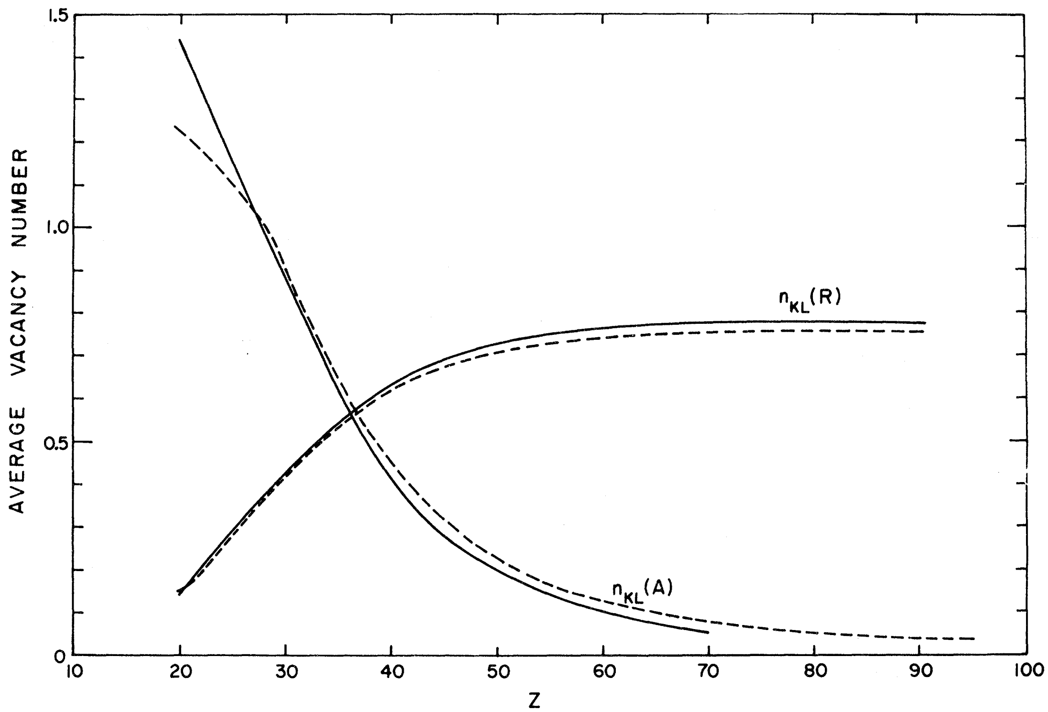

FIG. 10. Average number of L-shell vacancies due to Auger transitions $[n_{KL}(A)]$ and radiative transitions $[n_{KL}(R)]$ to the K shell, per K vacancy. The broken curves are computed from experimental data; the solid curves are derived from theory.

$$s_3 = \frac{I(L_3 \to N) + I(L_3 \to 0) + \cdots}{I(L_3 \to M)} = \frac{\text{Intensity of } L\beta \text{ x rays originating from } L_3 \text{ vacancies}}{\text{Intensity of } Ll \text{ and } L\alpha \text{ x rays originating from } L_3 \text{ vacancies}} . \quad (16)$$

If we take ω_K from a best fit to experimental data,[128] the $K\beta_1'/K\alpha_1$ intensity ratio from the review of Nelson, Saunders, and Salem,[129] and the $K\alpha_2/K\alpha_1$ and $K\beta/K\alpha$ ratios from the fit to experimental data listed in Table VI, and substitute these in Eq. (12), we find "experimental" values of $n_{KM}(R)$ that agree to within 7% or better with the theoretical results listed in Table VIII. For example, we find $n_{KM}(R)_{\text{expt}} = 0.0347$ for $Z=26$, 0.0857 for $Z=36$, 0.123 for $Z=47$, 0.140 for $Z=56$, and 0.151 for $Z=65$.

Experimental data that permit calculation of $n_{L_iM}(R)$ are only available for a few elements. Taking the branching ratios s_i from Venugopala Rao, Palms, and Wood[125] and fluorescence yields ω_i from McGeorge, Freund, and Fink,[130] Eq. (13) yields $n_{L_2M}(R)_{\text{expt}} = 0.133 \pm 0.030$ and $n_{L_3M}(R)_{\text{expt}} = 0.161 \pm 0.029$ for $Z=65$. For $Z=73$, with the ω_i of Mohan *et al.*,[131] we find $n_{L_2M}(R)_{\text{expt}} = 0.209 \pm 0.016$ and $n_{L_3M}(R)_{\text{expt}} = 0.192 \pm 0.016$. For $Z=80$, we have measurements of ω_i due to Palms *et al.*[132] that lead to $n_{L_2M}(R)_{\text{expt}} = 0.260 \pm 0.014$ and $n_{L_3M}(R)_{\text{expt}} = 0.247 \pm 0.014$. Only for $Z=82$ have the fluorescence yields of all three L subshells been measured,[125] leading to $n_{L_1M}(R)_{\text{expt}} = 0.067 \pm 0.057$, $n_{L_2M}(R)_{\text{expt}} = 0.291 \pm 0.024$, and $n_{L_3M}(R)_{\text{expt}} = 0.258$

TABLE VI. X-ray intensity ratios derived from a least-squares fit to the experimental data of Refs. 115–127.

Z	$I(K\alpha_2)/I(K\alpha_1)$	$I(K\beta)/I(K\alpha)$	Z	$I(K\alpha_2)/I(K\alpha_1)$	$I(K\beta)/I(K\alpha)$
20	0.503	0.128	58	0.545	0.241
22	0.504	0.133	60	0.548	0.246
24	0.505	0.133	62	0.552	0.250
26	0.507	0.134	64	0.555	0.254
28	0.508	0.135	66	0.559	0.257
30	0.510	0.135	68	0.563	0.261
32	0.512	0.148	70	0.567	0.264
34	0.514	0.158	72	0.571	0.267
36	0.516	0.168	74	0.575	0.270
38	0.518	0.177	76	0.579	0.272
40	0.520	0.185	78	0.583	0.275
42	0.522	0.193	80	0.588	0.277
44	0.525	0.201	82	0.592	0.279
46	0.527	0.208	84	0.597	0.281
48	0.530	0.214	86	0.602	0.283
50	0.533	0.220	88	0.607	0.285
52	0.536	0.226	90	0.612	0.287
54	0.539	0.231	92	0.617	0.288
56	0.542	0.236	94	0.622	0.290

TABLE VII. Average number of primary L_i subshell vacancies produced by transitions to the K shell: $n_{KL_i}(A)$ due to Auger transitions and $n_{KL_i}(R)$ due to radiative transitions. Also listed is the total number of primary L vacancies produced by Auger transitions $[n_{KL}(A)]$, by radiative transtions $[n_{KL}(R)]$, and by all transitions (n_{KL}) to the K shell.

Z	$n_{KL_1}(A)$	$n_{KL_2}(A)$	$n_{KL_2}(R)$	$n_{KL_3}(A)$	$n_{KL_3}(R)$	$n_{KL}(A)$	$n_{KL}(R)$	n_{KL}
20	0.234	0.725	0.048	0.492	0.096	1.451	0.144	1.595
22	0.223	0.640	0.065	0.491	0.129	1.354	0.194	1.548
24	0.214	0.559	0.083	0.474	0.165	1.247	0.248	1.495
26	0.201	0.485	0.103	0.447	0.203	1.133	0.306	1.439
28	0.185	0.415	0.123	0.410	0.242	1.010	0.365	1.375
30	0.170	0.353	0.142	0.372	0.279	0.895	0.421	1.316
32	0.154	0.298	0.159	0.333	0.311	0.785	0.470	1.255
34	0.139	0.252	0.175	0.294	0.340	0.685	0.515	1.200
36	0.125	0.212	0.188	0.259	0.365	0.596	0.553	1.149
38	0.112	0.178	0.200	0.227	0.387	0.517	0.587	1.104
40	0.0999	0.150	0.211	0.198	0.405	0.448	0.616	1.064
42	0.0897	0.126	0.220	0.173	0.421	0.389	0.641	1.030
44	0.0805	0.107	0.227	0.152	0.433	0.340	0.660	1.000
46	0.0722	0.0906	0.234	0.133	0.443	0.296	0.677	0.963
48	0.0653	0.0775	0.240	0.117	0.452	0.260	0.692	0.952
50	0.0588	0.0664	0.245	0.102	0.460	0.227	0.705	0.932
52	0.0533	0.0573	0.249	0.0893	0.465	0.200	0.714	0.914
54	0.0484	0.0507	0.253	0.0782	0.469	0.177	0.722	0.899
56	0.0441	0.0452	0.256	0.0688	0.473	0.158	0.729	0.887
58	0.0405	0.0405	0.259	0.0608	0.475	0.142	0.734	0.876
60	0.0372	0.0364	0.261	0.0538	0.477	0.127	0.738	0.865
62	0.0342	0.0327	0.264	0.0475	0.479	0.114	0.743	0.857
64	0.0320	0.0299	0.266	0.0429	0.479	0.105	0.745	0.850
66	0.0298	0.0272	0.268	0.0382	0.480	0.0952	0.748	0.843
68	0.0278	0.0249	0.270	0.0344	0.479	0.0871	0.749	0.836
70	0.0258	0.0226	0.272	0.0306	0.480	0.0790	0.752	0.831
72	0.0243	0.0208	0.274	0.0276	0.479	0.0727	0.753	0.826
74	0.0231	0.0195	0.275	0.0252	0.478	0.0678	0.753	0.821
76	0.0214	0.0176	0.277	0.0223	0.478	0.0613	0.755	0.816
78	0.0207	0.0168	0.278	0.0206	0.477	0.0581	0.755	0.813
80	0.0194	0.0154	0.280	0.0185	0.476	0.0533	0.756	0.809
82	0.0186	0.0145	0.281	0.0169	0.475	0.0500	0.756	0.806
84	0.0178	0.0136	0.284	0.0153	0.474	0.0467	0.758	0.805
86	0.0169	0.0127	0.285	0.0139	0.473	0.0435	0.758	0.802
88	0.0160	0.0118	0.286	0.0124	0.472	0.0402	0.758	0.798
90	0.0151	0.0109	0.288	0.0111	0.470	0.0371	0.758	0.795
92	0.0147	0.0105	0.289	0.0102	0.469	0.0354	0.758	0.793
94	0.0150	0.0105	0.290	0.0098	0.467	0.0353	0.757	0.792

±0.021. In summary, there is satisfactory agreement between theoretical and experimental values of $n_{L_iM}(R)$.

Auger-electron intensity ratios from which empirical M-vacancy production rates could be derived have unfortunately not yet been measured. Estimates of $n_{LM}(A)$ by Freund and Fink,[133] based on data of Haynes, Velinsky, and Velinsky[110] for $Z=83$, seem to indicate reasonable agreement with theory. However, a detailed comparison will only be possible when the high-resolution L-Auger electron data become available that are to be expected from ESCA (electron-spectroscopy-for-chemical-analysis) techniques.

VIII. CONCLUDING REMARKS

This work pertains to vacancy distributions that arise in the decay of single inner-shell vacancies only. Multiple inner-shell ionization produced, for example, by heavy-ion bombardment,[134] leads to different decay processes that are not yet well understood.[135] Furthermore, only ordinary radiationless transitions are considered, in which a single Auger electron is emitted. However, a double Auger process is known to occur with considerable probability, resulting in the ejection of two elec-

TABLE VIII. Probability of producing a primary M-shell vacancy through Auger transitions [$n_{KM}(A+CK)=n_{KM}(A)+n_{KM}(CK)$] and radiative transitions [$n_{KM}(R)$] to a K-shell vacancy, and through Auger transitions [$n_{L_iM}(R)$] to an L_i-subshell vacancy, derived from theory.

Z	$n_{KM}(A+CK)$	$n_{KM}(R)$	$n_{L_1M}(A+CK)$	$n_{L_1M}(R)$	$n_{L_2M}(A+CK)$	$n_{L_2M}(R)$	$n_{L_3M}(A+CK)$	$n_{L_3M}(R)$
16	0.201	0.0033						
20	0.221	0.0149						
22	0.212	0.0216						
24	0.197							
26	0.180	0.0371			1.863		1.937	
28	0.162				1.828			
29					1.819	0.0036	1.922	0.0039
30	0.144	0.0532						
32	0.128	0.0624			1.840			
33			1.084		1.764		1.839	
34					1.696			
35					1.612			
36	0.102	0.0806	1.167	0.0020	1.542	0.0118	1.697	0.0122
37					1.488	0.0132		
40	0.0790	0.0967	1.031	0.0034	1.415	0.0187	1.616	0.0197
42	0.0693	0.104	1.014	0.0054	1.402	0.0236	1.602	0.0250
47	0.0499	0.119	0.942	0.0084	1.349	0.0392	1.560	0.0409
50	0.0411	0.126	0.905	0.0105	1.304	0.0502		
51			0.762	0.0255	1.284	0.0545	1.497	0.0560
54	0.0318							
56	0.0281	0.137	0.673	0.0350	1.212	0.0779	1.384	0.0713
58	0.0249							
60	0.0221	0.143	0.666	0.0468	1.145	0.102	1.360	0.103
65	0.0166	0.149			1.074	0.141	1.284	0.137
67			0.614	0.0625				
70	0.0132	0.154	0.582	0.0865				
74			0.561	0.106	0.936	0.227	1.138	0.212
80			0.707	0.0730	0.819	0.288	1.024	0.265
85			0.681		0.721		0.929	
93					0.629		0.782	

trons from the outermost valence shell.[136] For light elements, this process can be expected to modify the probability of M-vacancy creation predicted in the present work to an extent that cannot yet be accurately assessed.

The survey of experimental and theoretical information included in this article clearly shows the need for much further work on this interesting subject.

ACKNOWLEDGMENTS

We are indebted to Dr. P. J. Ebert of the Lawrence Radiation Laboratory, Livermore, Dr. C. A. Quarles of Texas Christian University, and Dr. O. Schult of the Technische Universität München for results of their x-ray intensity measurements, and to Dr. E. J. McGuire of the Sandia Laboratories for his unpublished theoretical K-MN Auger rates.

*Work supported in part by the U. S. Atomic Energy Commision and by USAROD Basic Research Grants No. DA-ARO-D31-124-70-G78 and DA-ARO-D31-124-72-G39.

†Permanent address: Department of Physics, Emory University, Atlanta, Ga. 30322.

[1]M. A. Listengarten, Bull. Acad. Sci. USSR, Phys. Ser. 24, 1050 (1960).

[2]A. H. Wapstra, G. J. Nijgh, and R. van Lieshout, *Nuclear Spectroscopy Tables* (North-Holland, Amsterdam, 1959).

[3]R. W. Fink, R. C. Jopson, Hans Mark, and C. D. Swift, Rev. Mod. Phys. 38, 513 (1966).

[4]J. H. Scofield, Phys. Rev. 179, 9 (1969).

[5]V. O. Kostroun, M. H. Chen, and B. Crasemann, Phys. Rev. A 3, 533 (1971).

[6]M. H. Chen, B. Crasemann, and V. O. Kostroun, Phys. Rev. A 4, 1 (1971).

[7]B. Crasemann, M. H. Chen, and V. O. Kostroun, Phys. Rev. A 4, 2161 (1971).

[8]E. J. McGuire, Phys. Rev. A 2, 273 (1970).

[9]E. J. McGuire, Phys. Rev. A 3, 587 (1971).

[10]E. J. McGuire, Phys. Rev. A 3, 1801 (1971).

[11]B. Crasemann, M. H. Chen, and V. O. Kostroun, University of Oregon Nuclear Physics Report No. RLO-1925-53, 1971 (unpublished).

[12]W. N. Asaad, Nucl. Phys. 44, 399 (1963).

[13]W. N. Asaad, Nucl. Phys. 66, 494 (1965).
[14]W. Mehlhorn and W. N. Asaad, Z. Physik 191, 231 (1966).
[15]D. J. Ramsdale, Ph.D. thesis (Kansas State University, 1969) (unpublished).
[16]R. G. Albridge and J. M. Hollander, Nucl. Phys. 27, 554 (1961).
[17]R. G. Albridge, K. Hamrin, G. Johansson, and A. Fahlman, Z. Physik 209, 419 (1968).
[18]T. Azuma, J. Phys. Soc. Japan 9, 443 (1954).
[19]M. I. Babenkov and B. V. Bobykin, Bull. Akad. Sci. USSR, Phys. Ser. 32, 1840 (1968).
[20]J. B. Bellicard and A. Moussa, J. Phys. Radium 18, 115 (1957).
[21]J. Bellicard, A. Moussa, and S. Haynes, Nucl. Phys. 3, 307 (1957).
[22]I. Bergström, Arkiv Fysik 5, 191 (1952).
[23]I. Bergström and R. D. Hill, Arkiv Fysik 8, 21 (1954).
[24]B. V. Bobykin and N. I. Novik, Izv. Akad. Nauk SSSR, Ser. Fiz. 21, 1556 (1957).
[25]V. Brabets, K. Gromov, B. Dzhelepov, and V. Morozov, Izv. Akad. Nauk SSSR, Ser. Fiz. 23, 812 (1959).
[26]C. D. Broyles, D. A. Thomas, and S. K. Haynes, Phys. Rev. 89, 715 (1953).
[27]A. O. Buford, J. B. Perkins, and S. K. Haynes, Phys. Rev. 99, 3 (1956).
[28]W. R. Casey and R. G. Albridge, Z. Physik 219, 216 (1969).
[29]B. Cleff and W. Mehlhorn, Z. Physik 219, 311 (1969).
[30]J. M. Cork, M. K. Brice, D. W. Martin, L. C. Schmid, and R. G. Helmer, Phys. Rev. 101, 1042 (1956).
[31]J. S. Dionisio, Compt. Rend. 253, 2933 (1961).
[32]J. S. Dionisio, Compt. Rend. 254, 1972 (1962).
[33]J. S. Dionisio, Compt. Rend. 254, 257 (1962).
[34]J. S. Dionisio, Compt. Rend. 254, 3851 (1962).
[35]J. S. Dionisio, Ann. Phys. (Paris) 9, 29 (1964).
[36]B. S. Dzhelepov, B. K. Preobrazhenskii, I. M. Rogachev, and P. A. T. Shkin, Izv, Akad. Nauk SSSR, Ser. Fiz. 22, 126 (1958).
[37]B. S. Dzhelepov, B. K. Preobrazhenskii and V. A. Sergienko, Izv. Akad. Nauk SSSR, Ser. Fiz. 22, 945 (1959).
[38]C. D. Ellis, Proc. Roy. Soc. (London) A138, 318 (1932).
[39]C. D. Ellis, Proc. Roy. Soc. (London) A143, 350 (1934).
[40]P. Erman and Z. Sujkowski, Arkiv Fysik 20, 209 (1961).
[41]P. Erman, J. Rossi, E. C. O. Bonacalza, and J. Miskel, Arkiv Fysik 26, 135 (1964).
[42]P. Erman, I. Bergström, Y. Y. Chu, and G. T. Emery, Nucl. Phys. 62, 401 (1965).
[43]G. T. Ewan, Can. J. Phys. 35, 672 (1957).
[44]G. T. Ewan, R. L. Graham, and L. Grodzins, Can. J. Phys. 38, 163 (1960).
[45]G. T. Ewan, J. S. Geiger, R. L. Graham, and D. R. MacKenzie, Can. J. Phys. 37, 174 (1959).
[46]G. T. Ewan, J. S. Geiger, R. L. Graham, and D. R. McKenzie, Phys. Rev. 116, 950 (1959).
[47]G. T. Ewan and J. S. Meritt, Can. J. Phys. 38, 324 (1960).
[48]A. Fahlman, R. Nordberg, C. Nordling, and K. Siegbahn, Z. Physik 192, 476 (1966).
[49]M. Ference, Phys. Rev. 51, 720 (1937).
[50]R. N. Forrest and H. T. Easterday, Phys. Rev. 112, 950 (1959).
[51]M. S. Freedman, F. T. Porter, and F. Wagner, Phys. Rev. 151, 886 (1966).
[52]A. Fahlman, K. Hamrin, G. Axelson, C. Nordling, and K. Siegbahn, Z. Physik 192, 484 (1966).
[53]C. J. Gallagher, D. Strominger, and J. P. Unik, Phys. Rev. 110, 725 (1958).
[54]P. R. Gray, Phys. Rev. 101, 1306 (1956).
[55]R. L. Graham and J. S. Meritt, Can. J. Phys. 39, 1058 (1961).
[56]R. L. Graham, F. Brown, G. T. Ewan, and J. Uhler, Can. J. Phys. 39, 1086 (1961).
[57]R. L. Graham, I. Bergström, and F. Brown, Nucl. Phys. 39, 107 (1962).
[58]E. Grigorév, A. Zolotavin, V. Klementév, and R. Sinitsyn, Izv. Akad. Nauk SSSR, Ser. Fiz. 23, 159 (1959).
[59]K. Y. Gromov, B. S. Dzhelepov, A. G. Dmitriev, and B. K. Preobrazhenskii, Izv. Akad. Nauk SSSR, Ser. Fiz. 22, 153 (1958).
[60]C. J. Herrlander, R. Stockendal, and R. K. Gupta, Arkiv Fysik 17, 315 (1960).
[61]O. Hörnfeldt, A. Fahlman, and C. Nordling, Arkiv Fysik 23, 155 (1962).
[62]O. Huber, F. Humbel, H. Schneider, and A. de-Shalit, Helv. Phys. Acta 25, 3 (1952).
[63]G. Kaye, Nucl. Phys. 68, 529 (1965).
[64]H. Körber and W. Mehlhorn, Z. Physik 191, 217 (1966).
[65]F. A. Johnson and J. S. Foster, Can. J. Phys. 31, 469 (1953).
[66]R. Johnston, J. H. Douglas, and R. G. Albridge, Nucl. Phys. A91, 505 (1967).
[67]B. Jung and J. Svedberg, Nucl. Phys. 20, 630 (1960).
[68]R. J. Krisciokaitis and S. K. Haynes, Nucl. Phys. A104, 466 (1967).
[69]J. Laberrigue-Frolow and P. Radvanyi, J. Phys. Radium 17, 944 (1956); Compt. Rend. 242, 901 (1953).
[70]Y. Y. Lui and R. G. Albridge, Nucl. Phys. A92, 139 (1967).
[71]P. Marguin and M. A. Moussa, J. Phys. Radium 21, 149 (1960).
[72]P. Marguin and M. A. Moussa, J. Phys. Radium 21, 17 (1960).
[73]W. Mehlhorn and R. G. Albridge, Z. Physik 175, 506 (1963).
[74]M. Mladjenović and H. Slätis, Arkiv Fysik 8, 65 (1954).
[75]M. Mladjenović and H. Slätis, Arkiv Fysik 9, 41 (1955).
[76]J. C. Nall, Q. L. Baird, and S. K. Haynes, Phys. Rev. 118, 1278 (1960).
[77]J. O. Newton, Phys. Rev. 117, 1529 (1960).
[78]T. O. Passell, M. C. Michael, and I. Bergström, Phys. Rev. 95, 999 (1954).
[79]J. F. Perkins and S. K. Haynes, Phys. Rev. 92, 687 (1953).
[80]L. Persson, H. Ryde, and K. Oelsner-Ryde, Arkiv Fysik 21, 193 (1961).
[81]E. Plassmann and F. R. Scott, Phys. Rev. 84, 156 (1951).
[82]H. Ryde, L. Persson, and K. Oelsner-Ryde, Arkiv Physik 23, 171 (1962).
[83]F. R. Scott, Phys. Rev. 84, 659 (1951).
[84]E. Sokolowski and C. Nordling, Arkiv Fysik 14, 557 (1959).

[85]H. Slätis, Arkiv Fysik 37, 25 (1968).
[86]R. M. Steffen, O. Huber, and F. Humbel, Helv. Phys. Acta 22, 167 (1949).
[87]R. Stockendal, Arkiv Fysik 17, 553 (1960).
[88]Z. Sujkowski, Arkiv Fysik 20, 243 (1961).
[89]T. Suter and P. Reyes-Suter, Arkiv Fysik 20, 393 (1961).
[90]L. H. Toburen and R. G. Albridge, Nucl. Phys. A90, 529 (1967).
[91]J. Valentin, Compt. Rend. 254, 858 (1962).
[92]J. L. Wolfson and A. P. Baerg, Can. J. Phys. 42, 1781 (1964).
[93]T. Yuasa, Physica 18, 1267 (1952).
[94]M. J. Zender, W. Pou, and R. G. Albridge, Z. Physik 218, 245 (1969).
[95]A. I. Zernovoi, E. M. Krisiuk, G. D. Latyshev, A. S. Remennyi, A. G. Sergeev, and V. I. Sadeev, Zh. Eksperim. i Teor. Fiz. 32, 682 (1957) [Sov. Phys. JETP 5, 563 (1957)].
[96]I. Gizon and J. Boutet, Nucl. Phys. A103, 9 (1967).
[97]It should, however, be noted that fluorescence yields derived from some of the nonrelativistic calculations do, somewhat surprisingly, agree extremely well with experiment (see, e.g., Refs. 5–7).
[98]O. Hörnfeldt, Arkiv Fysik 23, 235 (1962).
[99]E. J. McGuire (private communication).
[100]C. P. Bhalla, H. R. Rosner, and D. J. Ramsdale, J. Phys. B 3, 1232 (1970).
[101]W. N. Asaad and E. H. S. Burhop, Proc. Phys. Soc. (London) 71, 369 (1958).
[102]W. Mehlhorn, Z. Physik 208, 1 (1968).
[103]W. Mehlhorn and D. Stalherm, Z. Physik 217, 294 (1968).
[104]M. O. Krause, Phys. Letters 19, 14 (1965).
[105]J. Gizon, A. Gizon, and J. Valentin, Nucl. Phys. A120, 321 (1968).
[106]R. Päschke, Z. Physik 176, 143 (1963).
[107]J. Burde and S. G. Cohen, Phys. Rev. 104, 1085 (1956).
[108]Z. Sujkowski and O. Melin, Arkiv Fysik 20, 193 (1961).
[109]K. Risch, Z. Physik 159, 89 (1960).
[110]S. K. Haynes, M. Velinsky, and L. J. Velinsky, Nucl. Phys. A90, 573 (1967).
[111]K. Risch, Z. Physik 150, 87 (1958).
[112]Z. Sujkowski and H. Slätis, Arkiv Fysik 14, 101 (1958).
[113]S. Aksela, M. Pessa, and M. Karras, Z. Physik 237, 381 (1970).
[114]H. R. Rosner and C. P. Bhalla, Z. Physik 231, 347 (1970).
[115]G. C. Nelson and B. G. Saunders, Phys. Rev. 188, 108 (1969).
[116]P. J. Ebert and V. W. Slivinsky, Phys. Rev. 188, 1 (1969).
[117]P. J. Ebert (private communication).
[118]J. S. Hansen, H. U. Freund, and R. W. Fink, Nucl. Phys. A142, 604 (1970).
[119]J. S. Hansen, Ph.D. thesis (Georgia Institute of Technology, 1971) (unpublished).
[120]A. G. de Pinho, Phys. Rev. A 3, 905 (1971).
[121]O. B. Schult, Z. Naturforsch. 26, 368 (1971), and private communication.
[122]S. I. Salem and R. J. Wimmer, Phys. Rev. A 2, 1121 (1970).
[123]V. D. Mistry and C. A. Quarles, Nucl. Phys. A164, 219 (1971).
[124]C. A. Quarles (private communication).
[125]P. Venugopala Rao, J. M. Palms, and R. E. Wood, Phys. Rev. A 3, 1568 (1971).
[126]L. M. Middleman, R. L. Ford, and R. Hofstadter, Phys. Rev. A 2, 1429 (1970).
[127]P. Richard, T. I. Bonner, T. Furuta, and I. L. Morgan, Phys. Rev. A 1, 1044 (1970).
[128]W. Bambynek, B. Crasemann, R. W. Fink, H. U. Freund, Hans Mark, R. E. Price, P. Venugopala Rao, and C. D. Swift (unpublished).
[129]G. C. Nelson, B. G. Saunders, and S. I. Salem, Atomic Data 1, 377 (1970).
[130]J. C. McGeorge, H. U. Fruend, and R. W. Fink, Nucl. Phys. A154, 526 (1970).
[131]S. Mohan, R. W. Fink, R. E. Wood, J. M. Palms, and P. Venugopala Rao, Z. Physik 239, 423 (1970).
[132]J. M. Palms, R. E. Wood, P. Venugopala Rao, and V. O. Kostroun, Phys. Rev. C 2, 592 (1970).
[133]H. U. Freund and R. W. Fink, Phys. Rev. 178, 1952 (1969).
[134]D. Burch and P. Richard, Phys. Rev. Letters 25, 983 (1970).
[135]M. E. Rudd, in *Proceedings of the VII International Conference on the Physics of Electronic and Atomic Collisions* (North-Holland, Amsterdam, 1971).
[136]T. A. Carlson and M. O. Krause, Phys. Rev. Letters 17, 1079 (1966).